Desalination and Water Treatment
www.deswater.com
doi: 10.1080/19443994.2016.1184185

57 (2016) 28122–28132
December

Taylor & Francis
Taylor & Francis Group

Seawater desalination by combined nanofiltration and ionic exchange

Rodrigo Bórquez*, Javier Ferrer

Chemical Engineering Department, University of Concepción, Concepción, Chile, Tel. +56 41 2204534; Fax: +56 41 2247491; emails: rborquez@udec.cl (R. Bórquez), jferrer@udec.cl (J. Ferrer)

Received 29 January 2014; Accepted 25 April 2016

ABSTRACT

This paper presents the experimental results to obtain drinking water from seawater by two alternatives: The first consists of two stages of nanofiltration in series, comparing different membranes of nanofiltration and reverse osmosis (RO) and second alternative is a stage of nanofiltration and another stage of ion exchange. Two stages of nanofiltration at transmembrane pressures (TMP) 40 and 20 bars, respectively, temperatures between 10 and 15°C, and feed flow between 707 and 1,325 L/h showed that 99.9% total dissolved solids (TDS) and Ca^{2+}, Cl^{-}, Mg^{2+}, Na^{+}, and SO_4^{2-} ions were removed, which meets the regulation of drinking water in Chile. This was possible by the nanofiltration membrane NF90–2540 which reduced TDS from 33.5 to 0.01 g/L, with 47.8 L/m^2 h permeate flux in first stage and 65.7 L/m^2 h in the second stage, this was much greater that 15.56–16.08 L/m^2 h in first and second stage, respectively, obtained with typical RO membranes operating at the same TMP. Optimal operating condition for nanofiltration is 10°C of temperature and feed flow of 1,325 L/h. However, one step of nanofiltration at 40 bar was unable to remove the required Cl^{-} and Na^{+} ions concentration to meet the Chilean and World Health Organization (WHO) drinking water regulations, therefore it is necessary to carry out second stage of ion exchange. For this stage, anionic resin Purolite A-300 and cationic resin Purolite C-100 were selected, given the high capacity obtained for these experimental, 1.35 meq/g for the anionic resin and 1.53 meq/g for the cationic resin, with rupture times around 115–150 min, respectively. Optimal operating condition is low feed flow (20 L/h) for an inlet concentration of 853 mg/l, for which retention of 94% of chloride and sodium ions is obtained and complies with Chilean regulations and the recommendations of the WHO.

Keywords: Nanofiltration; Ionic exchange; Seawater; Reverse osmosis

1. Introduction

Water scarcity is among the main problems to be faced by many societies and the world in the twenty-first century. Water use has been growing at more than twice the rate of the population increase in the last century, and, although there is no global water scarcity as such, an increasing number of regions are chronically short of water [1].

Chile is no stranger to this problem. Water has been reduced due to global warming and changes in the hydrological cycles. During the twentieth century, the country experienced a loss of more than 40% of its fresh water reserves, mainly in the North and Center. Meanwhile, the 4th report of the Intergovernmental Panel on Climate Change (IPCC) states that by 2040

*Corresponding author.

rainfall will decrease by 15% compared to the current date, causing a negative effect on agriculture, drinking water, process industries, energy sector, and others [2].

Desalination is considered as an attractive and reliable technology for making new water available from saline sources that forms 97.5% of the planet's water [3,4]. However, the conventional desalination technologies including the reverse osmosis (RO) process are often considered an energy-intensive process. RO desalination operates at a very high hydraulic pressure in order to overcome the osmotic pressure of the saline water and therefore requires significant energy. More energy is consumed since RO process is prone to membrane scaling and fouling problems [5–7]. Energy is a big issue because most energy sources are fossil fuel-based which directly contributes towards global warming and climate change, and therefore have further implications on the water scarcity issues [8–10].

Therefore it is necessary to seek other alternative desalination technologies which are sustainable over time, like the case of the nanofiltration, which has lower operation cost because of the use of lower operating pressures in comparison to RO, which implies a lower consumption energy [11].

In this work, therefore, higher salt concentrations, representative of seawater salinity, will be handled using three different commercial NF membranes. This will establish the viability of using NF membranes in the pretreatment step of desalination process. Towards this end, three different nanofiltration membranes (NF90, NF270, and NF30) and osmosis reverse membrane (RO98) are tested using a cross flow filtration cell. The effect of pressure on rejection and permeate flux for different high salt concentrations (NaCl) in raw seawater (up to 34,000 ppm) is determined.

1.1. Seawater desalination process and existent technologies

Seawater contains a variety of salts. Its high salinity prevents it use for human consumption, so it is necessary to reduce the salt load to comply with national and international standards for drinking water.

The increase in worldwide shortage of fresh water resources and recent reduction in the cost of desalination technologies have enhanced the interest in potable water production from saline waters. Generally desalination technologies may be grouped into thermal methods, i.e. multi-stage flash (MSF), multi-effect distillation (MED), and membrane processes, i.e. RO and electrodialysis (ED) [3–8]. Of the above methods, MSF, MED, and CV are economically inefficient, since having a medium-high energy consumption and high investment costs translating into high cost per unit of water treated and ED method has the drawback to purify brackish water only, so that the RO is the most convenient method, whereas the ion-exchange process provides high quality if the initial salt concentration is less than 1 g/L and is a convenient method when combined with any of the above processes.

Historically, most of installed seawater desalination capacity has been produced using thermal distillation processes. Since 1990s, RO membrane systems have become the fastest growing segment of the seawater desalination market. Actually, more than 14,000 plants produce over 65 million m^3 of desalinated water daily around the globe [12], principally in the Mediterranean, the Middle East, and USA's west coast. However, also the aforementioned methods, there are newer methods such as nanofiltration, which is based on a process of filtration through semipermeable membranes, NF membranes have been proposed as an alternative to RO membrane for desalting seawaters.

1.2. Reverse osmosis (RO) and nanofiltration (NF)

Seawater is characterized by having high degree of hardness, varying turbidity and bacterial contents, and high TDS. These properties give rise to major problems such as scaling, fouling, high-energy requirements, and the requirement of high quality construction materials. Conventional seawater thermal and/or membrane desalination processes are complex. To solve seawater desalination problems and to minimize their effects on productivity and water cost of conventional plants, nanofiltration membranes have recently been employed in pre-treatment facilities in both RO and thermal processes [13,14]. The NF membrane pretreatment was found to be successful in the removal of turbidity, residual bacteria, scale forming hardness ions, lowering of the seawater TDS, and reducing energy and chemical consumption [3]. This will enhance the production of desalted water and reduces its production cost; yet it is an environmentally friendly process. In addition, the correct choice of NF membrane is of vital importance for the pretreatment of seawater, which will make or break the economical feasibility of the whole process.

NF membranes have intermediate rejection rate between RO and ultrafiltration. Depending on the membrane structure, NF membranes have high rejection rate to divalent ions which exceeds 98% and average to low rejection rate to monovalent ions [3,9].

The permeability of NF membrane is several times higher than RO membranes. Therefore, the main advantage of NF membranes is the lower energy consumption compared to RO membranes.

A recent comprehensive review on the use of nanofiltration membranes in water treatment has been presented elsewhere [15]. Many researchers [16] studied the rejection of different salts (e.g. NaCl, $MgCl_2$, Na_2SO_4, $CaSO_4$, and $MgSO_4$) using different types of nanofiltration membranes.

Their results showed that the rejection values changed according to the type of the NF membranes used. Schaep et al. [17] found that the rejection of NaCl using NF40 membrane was about 45% and this rejection increased up to 55% using UTC 20 membrane at 10 bars. The rejection of divalent ions was about 95% for the two membranes.

Afonso et al. [18] had similar results for the rejection using Desal G-10 and Desal G-20 nanofiltration membranes, while the rejection of NaCl was low at around 15% using PE S5 nanofiltration membrane. However, the above studies were carried out at low salts concentrations.

The sudden flux decline during pressure-driven membrane processes is a result of concentration polarization and/or fouling. Concentration polarization arises due to the membrane perm-selectivity. Solutes are dragged to the membrane surface by convective transport of the solvent, a fraction of which may pass through the membrane, whereas the rejected solutes accumulate in the membrane vicinity and may form fairly viscous and gelatinous layers. The formation of a gel-layer or a secondary membrane reduces the flux and may also hinder the passage of low molecular weight solutes [19,20].

Fouling results from the deposition of submicron particles, as well as crystallization, precipitation, and adsorption solutes on the membrane surface or inside its pores. The extent of membrane fouling mainly depends on the nature of the membrane used and the feed characteristics. The first means for controlling this phenomenon is a careful choice of the membrane type. Secondly, a module design providing suitable hydrodynamic conditions for the particular application should be chosen. An adequate feed pretreatment is also fundamental [6].

As will be seen below, in a single-stage nanofiltration is not achieved the permissible limits set by current regulations for potable water, then is necessary to performing a second-stage nanofiltration or ion-exchange step. For example, combinations of RO and ion-exchange resins have been used for desalting seawater and specifically for boron removal [11]. If the boron is removed up to detection limit, the ion-exchange process is more economical than RO process. Black seawater has been softened using a combination of RO and resins process, for boiler waters production [21].

1.3. Ionic exchange

Ion exchange is a unit operation based on mass transfer between a solid and a liquid phase. It involves the transfer of one or more ions from the liquid to the solid phase by ion exchange or displacement of the same charge that are attached by electrostatic forces to surface functional groups. The process efficiency depends upon the solid–liquid equilibrium and mass transfer rate. The solids are generally of polymeric type, the most common being based on synthetic resins [22].

An ion-exchange resin can be considered a structure of hydrocarbon chains, which are attached rigidly to free ionic groups. These chains are joined transversely to form a three-dimensional matrix which provides rigidity to the resin and wherein the degree of crosslinking. Crosslinking determines the internal porous structure of it. As ions must diffuse inside the resin exchange, selecting the degree of crosslinking can be limited the mobility of the ions involved [23].

The charges of immobile ionic groups are balanced with other ions, of opposite sign, called counter ions, which are free and which are actually being exchanged with the dissolved electrolyte. The ion-exchange process may be represented as a reversible chemical reaction that takes place when a solution of an ion is exchanged for other ions of the same sign which is attached to an immobile solid particle, as shown in Eq. (1) [22]:

$$R - OH_{(s)} + B^-_{(I)} \leftrightarrow R - B_{(S)} + OH^-_{(I)} \quad (1)$$

Eq. (1) represents the reaction between a functional group whose resin is the hydroxyl ion and B^- represents the anions present in the aqueous solution.

The resin capacity is usually expressed in dry weight basis, wet weight, or volume of resin as meq retained solute/g resin or meq/ml [23]:

$$\text{Capacity} = -\frac{\text{Mass of exchanged solute}}{\text{Mass of resin}}\left(\frac{\text{meq}}{\text{g}}\right) \quad (2)$$

Capacity is a critical parameter for the selection of the ion exchanger, high capacity is generally required for to take place the separation or purification.

Time from the start of the operation in the bed until the dissolution ions appear in the output current, or more precisely, when it reaches the maximum permissible concentration in the effluent is called the rupture time (*tR*). At this time, the flow is diverted to a second bed, starting the regeneration process for the first bed. The rupture curves are usually of sigmoidal shape, but may have a steep slope or be relatively flat and, in some cases considerably distorted. If the adsorption process was infinitely fast, the rupture curve would be a straight vertical line. The actual speed and the mechanism of adsorption, the adsorption equilibrium, the fluid velocity, the solute concentration in the feed, the length of the ion-exchange bed, and particularly if the concentration of solute in the feed is high, will determine the shape of the curve produced in any system. Usually, the rupture time decreases with decreasing height of the bed, increases with the particle size of the adsorbent, decreases with fluid flow through the bed, and decreases with the initial solute content of the feed [22].

2. Material and methods

2.1. Microfiltration

Raw seawater was pretreated by microfiltration stage using "Kerasep" 0.1 μm inorganic tubular membrane (Rhodia-Orelis, France) in order to remove suspension particles. The operating conditions for microfiltration are 4 bar and ambient temperature.

2.2. Nanofiltration and RO membranes

(1) Alfa Laval Pilot Unit 2,5´´ RO/NF (www.alfalaval.com) was used for all the desalination experiments. The operating pressure was of 40 bar in the first stage and 20 bar in the second stage of nanofiltration, and operating temperatures between 10 and 15°C and feed flow between 707 and 1,325 L/h. A detailed schematic of the experimental process of nanofiltration and RO is presented in Fig. 1.
(2) Alfa Laval's RO99pht 2517/30, NF99 2517/48, NF99 HF-2517/30 and DOW's NF90-2540 membranes were used in the experiments with membrane surface area of 1, 0.7, 1.1 y 2.6 m^2, respectively, and spiral geometry type. For every membrane tested, the desalination process was performed in two successive stages shows in Fig. 1.
(3) Temperature and pressure variables were controlled and measured during the desalination process and permeate flux, conductivity, and salinity were measured for the desalinated water.
(4) Salinity analysis of desalinated water were performed using methods such as Volhard and Mohr method for chloride ions, gravimetric methods for sulfate ions, complex reaction formation methods for the determination of calcium ions, and magnesium and atomic adsorption spectrophotometry for sodium ions.

2.3. Ion-exchange desalination

(1) For the ion exchange, a semi-continuous setup using a serial process with cationic and anionic columns in order to obtain drinking water was used [11,21]. Two columns of 80 cm high and 10 cm diameter were used, and were filled with 4 L of resin. The salted water used for these experiments was the one obtained as the first stage of nanofiltration permeate (stream 3 in Fig. 2).
(2) The resins used in the experimental test were Purolite A-300, Purolite A-500, Rohm and Haas Amberlite IRA 458, Purolite MB-400, strongly basic resins, Purolite C-100 and Purolite C-100E, strongly acidic resins.
(3) The ion measurement was done by a conductivity meter connected to the output of the columns in order to obtain an approximate value of the saline content of the water in time. The measurements of total dissolved solids (TDS), sodium chloride (NaCl), and chloride and sodium ions were taken from the final sample to determine TDS, and sodium chloride (NaCl) selective electrode was used to determine the concentration of chloride and sodium ions by means of Volhard methods and atomic adsorption spectrophotometry, respectively [24].
(4) To determine the resin capacity, 25 ml of 1 M sodium chloride solution was used with 5 g of each in a glass beaker and stirred for 20 min until equilibrium was reached. Then, the samples of 5 ml of the final solutions were taken and the samples were analyzed with the above-mentioned methods.

3. Results

3.1. Microfiltration

Table 1 presents the concentration of salts feed and output of microfiltration pretreatment. It is observed that there is practically no reduction in the concentration of salts because the microfiltration retains larger particles, usually 0.02–10 μm such as colloids and emulsions, yeasts, bacteria, and virus.

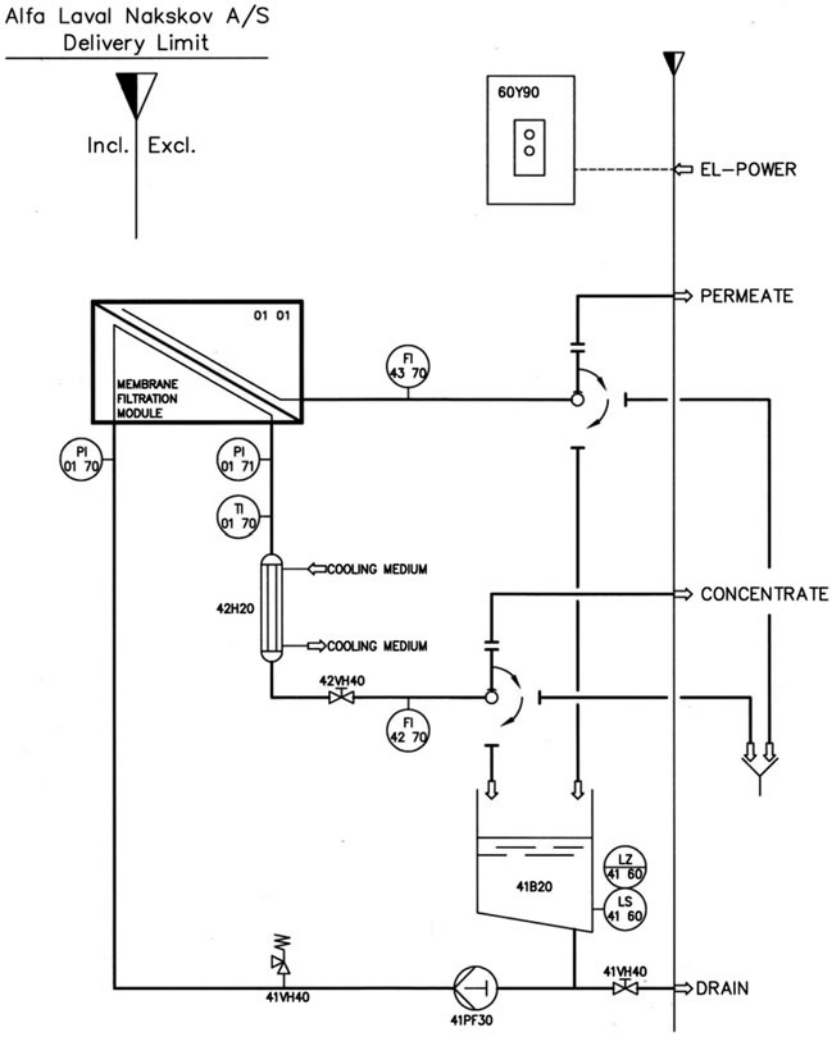

Fig. 1. Scheme of the experimental process of nanofiltration and reverse osmosis (RO).

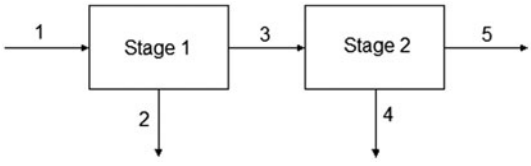

Fig. 2. Scheme for the two stage membrane (NF or RO) desalination process.
Notes: (1) pretreated seawater feed stream, (2) first stage retentate stream, (3) first stage permeate stream, (4) second stage retentate stream, and (5) second stage permeate stream (product).

3.2. Performance of nanofiltration and RO membranes

Results obtained from experimental tests of two stages in series with different membranes, nanofiltration as both RO to a pressure of 40 bar in the first stage and 20 bar for the second stage was compared.

Tables 2 and 3 show that membranes with most salt rejection and reduction in TDS were nanofiltration membrane NF90-2540 and RO membrane RO98pht 2517/30.

The membrane NF99 HF-2517/30 has the highest flux yield, but it has an extremely low salt rejection 66.5%, regarding membranes as NFX-2540 and RO98pht 2517/30, which provide greater retention than 99%.

On the other hand, even though RO membrane RO98pht 2517/30 has an elevated salt rejection, the permeate flow is 16 L/h m^2, almost three times lower than the flux of NF90-2540 of 65.7 L/h m^2 after the second stage. It is mainly due to the effect of

Table 1
Chemical composition of raw seawater and after microfiltration (4 bar, T = 25°C, Feed flow = 707 L/h)

	Raw seawater	Seawater after microfiltration
Conductivity (mS/cm)	48.1	47.6
TDS (g/l)	33.5	31.1
Nacl (g/l)	24	24
Na^+ (g/l)	10.26	10.76
Cl^- (g/l)	19.65	18.63
SO_4^{2-} (g/l)	2.68	2.57
Ca^{2+} (g/l)	0.41	0.39
Mg^{2+} (g/l)	1.26	1.22

Table 2
Permeate flux, dissolved salts concentration, and TDS in permeate by NF and RO after the first stage (40 bar, T = 15°C, Feed flow = 707 L/h)

Process/membrane	Permeate flux (L/h m^2)	TDS (mg/L)	Na^+ (mg/L)	Cl^- (mg/L)	SO_4^{2-} (mg/L)	Ca^{2+} (mg/L)	Mg^{2+} (mg/L)
Feed seawater		33,500	10,260	18,450	2,570	390	1,220
Reverse osmosis/RO98pht 2517/30	15.56	489.5	157.8	243.6	7.2	–	–
Nanofiltration/NF99 2517/48	67.88	18,150	2,420	14,190	280	–	–
Nanofiltration/NF99 HF-2517/30	148.52	16,100	1,950	13,200	240	130	230
Nanofiltration/NF90-2540	47.80	899	242	498	8.14	1.94	2.4
NCH 409[a]	–	1,500	–	400	500	–	125
WHO[b]	–	1,000	100	250	400	–	30

[a]Physicochemical limits according to Chilean drinking water standard (Nch 409).
[b]World Health Organization (WHO).

Table 3
Permeate flux, dissolved salts concentration, and TDS in permeate by NF or RO after the second stage (20 bar, T = 15°C, Feed flow = 707 L/h)

Process/membrane	Permeate flux (L/h m^2)	TDS (mg/L)	Na^+ (mg/L)	Cl^- (mg/L)	SO_4^{2-} (mg/L)	Ca^{2+} (mg/L)	Mg^{2+} (mg/L)
Reverse osmosis/RO98pht 2517/30	16.08	8.82	2.80	4.40	1.64		
Nanofiltration/NF99 2517/48	69.12	11,190	820	9,120	10		
Nanofiltration/NF99 HF-2517/30	95.15	9,020	1,030	6,960	10	20	60
Nanofiltration/NF90-2540	65.70	11.7	4	6	1.34	0.72	0.93
NCH 409[a]	–	1,500	–	400	500	–	125
WHO[b]	–	1,000	100	250	400	–	30

Notes: Feed concentrations are permeate concentrations indicated in Table 2.
[a]Physicochemical limits according to Chilean drinking water standard (Nch 409).
[b]World health organization (WHO).

osmotic pressure, which is lower in nanofiltration membranes, which implies an increased flow of permeate. Therefore, the nanofiltration membrane NFX-2540 meets the optimal conditions in terms of permeate flux and salt retention in two separation stages.

3.3. *Effects of pressure, temperature, and feed flow over performance of membrane NF90-2540*

Fig. 3 shows the relation of the permeate conductivity with the operation pressure and temperature. The tests were performed at feed flow of 706.7 L/h and temperatures of 15 and 10˚C, respectively.

From Fig. 3, it is possible to appreciate that operation temperature affects the salt diffusion because at higher temperatures the permeate conductivity increases, which means an increase in the dissolved salts in permeate.

Additionally, we can appreciate that at higher operation pressures the permeate conductivity diminishes, which means that salt rejection is increased by the pressure variations.

In the following figures, the relations of TDS, chloride, and sodium ion concentration in permeate with operating pressure is analyzed, considering different operating temperatures and feed flows.

Figs. 4 and 5 show the effect of operating temperature on the removal of ions, which clearly shows that increasing the temperature increases the concentration of TDS, chloride ions, and sodium ions in the permeate, since at higher temperature increases the diffusion of ions through the membrane. Furthermore, in Fig. 4 (feed 707 L/h, temperature 10˚C), we can appreciate the operating pressure effect on the salt rejection yield, where it increased with pressures above 34 bar, but in operation between 28 and 34 bar doesn't show this effect. On the other hand, this effect is not appreciated in Fig. 5 (feed 707 L/h, temperature 15˚C).

Figs. 5 and 6 show the effect of increased cross-feed flow across the membrane, which causes a decrease in the concentration of dissolved salts in the permeate, since as fluxes showing higher permeate cause greater dilution of salts. Thus, the flux and average rejection decreased with decreasing cross-flow velocity. This is due to the increased polarization

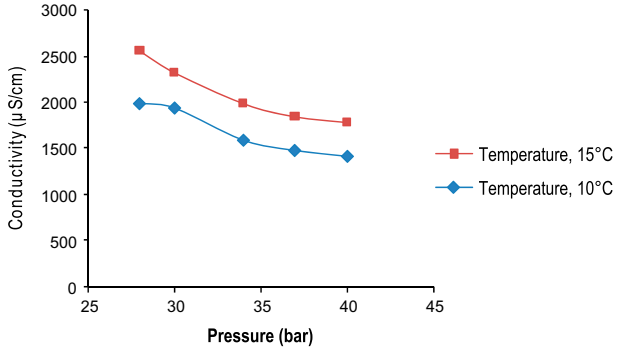

Fig. 3. Conductivity in permeate of first stage with membrane NF90-2540 against operating pressure to a seawater microfiltrated feed flow of 707 L/h.

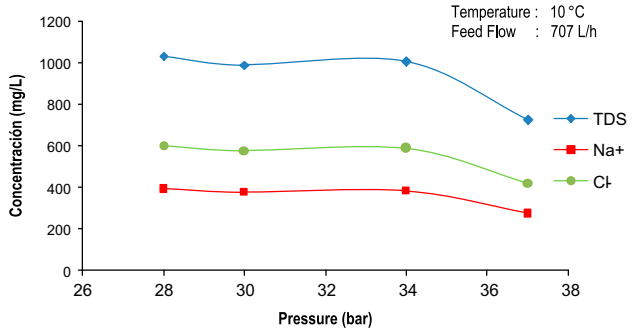

Fig. 4. Relations of TDS, chloride, and sodium ion concentration in permeate of first stage with membrane NF90-2540 against operating pressure to a seawater microfiltrated feed flow of 707 L/h and 10˚C.

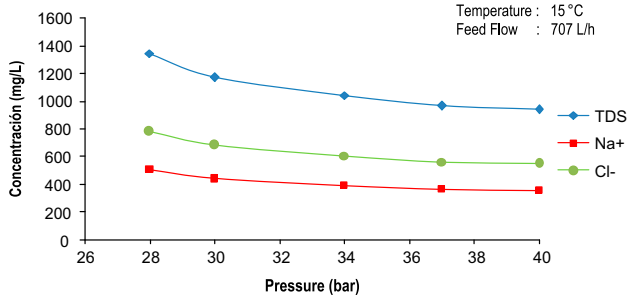

Fig. 5. Relations of TDS, chloride, and sodium ion concentration in permeate of first stage with membrane NF90-2540 against operating pressure to a seawater microfiltrated feed flow of 707 L/h and 15˚C.

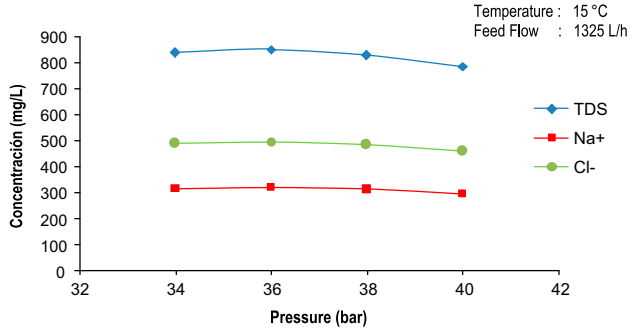

Fig. 6. Relations of TDS, chloride, and sodium ion concentration in permeate of first stage with membrane NF90-2540 against operating pressure to a seawater microfiltrated feed flow of 1,325 L/h and 15˚C.

modulus, with a higher ion concentration at the membrane surface, both solutes diffuse through the membrane and osmotic pressure will increase; this will result in lower TDS rejection and permeate flux [14–16].

Fig. 7 shows the rejection yield of the membrane for different ions in the salted water. Here we can see that with bivalent ions like Calcium, Magnesium, and higher sulfates the rejection yield is above 99%. On the other hand, with monovalent ions like chloride and sodium, the rejection does not exceed 98%, which is still much higher than the yields performed by the other NF membranes NF99 2517/48 and NF99 HF-2517/30 that weren't higher than 82%.

Rejection generally increases with pressure because more water flows through the membrane with approximately the same amount of salt. However, for some of the salts, a maximum rejection was observed beyond which rejection decreased with increasing pressure. This phenomenon likely occurs because as pressure increases, both the flux and polarization modulus also increase, but at different rates. At some point, the effects of the increased polarization modulus will overcome the effects of the increased flux and the rejection will decrease [14,15,18].

From the above trials, it can be concluded that the three operating variables (pressure, temperature, and permeate flow) exert different influence on NF recovery and product quality. Increasing feed pressure increases both permeate flow as well as recovery and improves its quality. Improvement in permeate flow and recovery can be achieved also by increasing feed temperature which leads to a moderate decline in permeate quality. Increasing feed flow improves both permeate flow and quality but it has a marked influence on lowering permeate recovery. Those operation criteria are being investigated thoroughly for the proper operation of large NF plants by this NF-seawater desalination process [14,15,18].

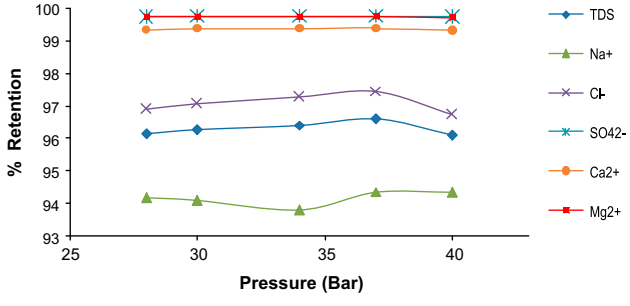

Fig. 7. Ion rejection percentage during first stage with membrane NF90-2540 against operating pressure to feed flow of 1,325 L/h and 15°C.

3.4. Experimental results of ion exchange

The removal of chloride ions and sodium was studied by a second stage of ion exchange, since a single-stage nanofiltration does not remove sufficient amount of chloride and sodium ions to comply with current Chilean regulations and the recommendations of the World Health Organization (WHO).

The performance of four strongly basic resins Purolite A-300, Purolite A-500, Purolite MB-400 and Rohm and Haas Amberlite IRA 458 for reduction of chloride ions were analyzed, while in the case of the strongly acidic resins Purolite C-100 and Purolite C-100E were selected for reducing sodium ion.

3.5. Experimental results of Ion-exchange resin capacity

Tables 4 and 5 summarize the initial and final chloride and sodium ion concentration, additionally the experimental average capacity and the theoretical capacity for the tested resins. From Tables 4 and 5, the highest capacity resins are Purolite MB-400 and Purolite A-300 in the case of the strongly basic and Purolite C-100 for the strongly acidic ones. Furthermore, it is observed that the capacity experimentally obtained is less than the theoretical capacity, since the theoretical capacity is the total capacity of the resin, which is an ideal case where the resin is completely at the beginning of the cycle. This case does not exist in reality, because the front of exchange is not flat and the resin is not always completely regenerated at the beginning of the cycle. The typical useful capacity of the strongly acidic and basic resins is 40–70% of its total capacity.

3.6. Rupture curves for ionic exchange resins

The realization of breakthrough curves was made using resins with greater capacity [25–27]. Fig. 8 shows the rupture curves experimentally obtained for anionic exchange columns.

For resin Purolite A-300, rupture time is 115 min and for Purolite MB-400 is 45 min. This is explained because Purolite MB-400 shares both cationic and anionic active sites, which reduces the rupture time.

The figure also shows the elevated chloride ion retention capacity both resins have. Purolite A-300 reaches concentration up to 17.3 mg/L and Purolite MB-400 reaches 12.56 mg/L, which agrees with the

Table 4
Experimental and theoretical capacity of strongly basic ion-exchange resins

	Purolite A-300	Purolite A-500	Purolite MB-400	Amberlite IRA 458
$(Cl^-)_{initial}$, mg/L	887.5	887.5	887.5	887.5
$(Cl^-)_{final}$, mg/L	649	691	644	705
Capacity (wet), mg/g resin	47.7	39.3	48.7	36.5
Capacity (wet), meq/g resin	1.35	1.07	1.38	1.03
Theoretical capacity (wet), meq/g resin	1.867	1.643	1.805	1.736

Table 5
Experimental and theoretical capacity of strongly acidic ion-exchange resins

	Purolite C-100	Purolite C-100E
$(Na^+)_{initial}$, mg/L	575	575
$(Na^+)_{final}$, mg/L	399.5	397.5
Capacity (wet), mg/g resin	35.1	33.5
Capacity (wet), meq/g resin	1.53	1.46
Theoretical capacity (wet), meq/g	2.35	2.24

experimental data obtained in section resin capacity of ion exchange. Similar curve was obtained for cationic ion-exchange columns (Fig. 9), Purolite C-100 resin has a rupture time of 150 min.

3.7. Semi-continuous fixed bed operation

For the experimental tests 4 L of anion resin Purolite A-300 and 4 L of cation resin Purolite C-100 were used. Fig. 10 shows the variation in salted water conductivity with time during the ionic exchange stage.

From Fig. 10, it is observed that the stationary state reached at approximately 10 min of operation, reaching an average conductivity of 107.5 μS/cm, which indicates low salt content present in the output water.

Table 6 shows TDS, sodium chloride, chloride, and sodium ion concentrations in the feed and the exit of the ionic exchange columns and their respective retention percentages. We can appreciate the high yield of salt retention and product from this process exceeds the requirements for the Chilean and WHO drinking water standards.

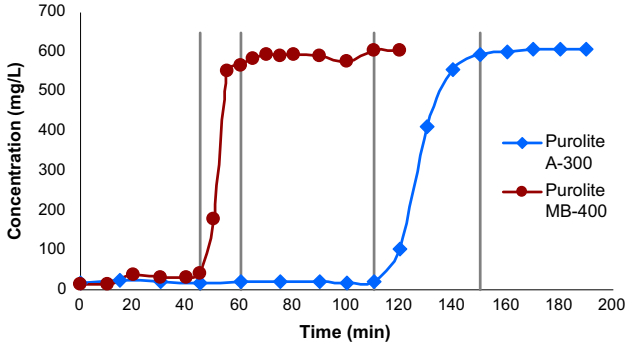

Fig. 8. Breakthrough curve for 1 g/l sodium chloride solution (600 ppm of Cl^-) with a volumetric flow of 15 ml/min in two basic resins.

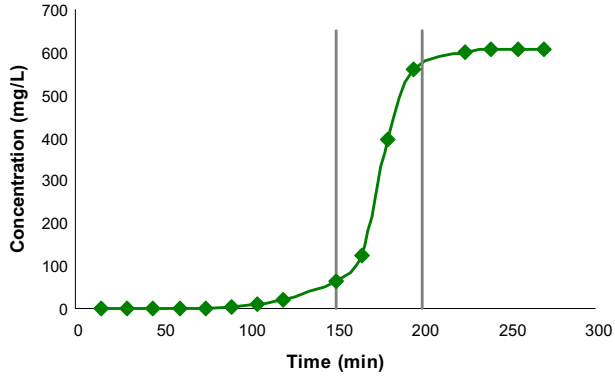

Fig. 9. Breakthrough curve for 1 g/l sodium chloride solution (400 ppm of Na^+) with a volumetric flow of 15 ml/min in acid resin Purolite C-100.

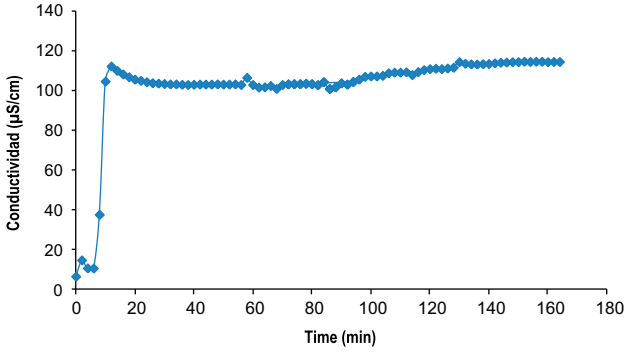

Fig. 10. Water conductivity at the exit of the ionic exchange process vs. time with a feed flow of 20 L/h of permeate from first stage with membrane NF90-2540 at 40 bar, and an initial conductivity of 1,700 µS/cm.

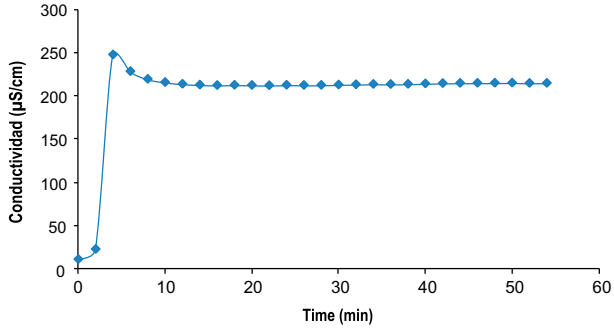

Fig. 11. Water conductivity at the exit of the ionic exchange process vs. time with a feed flow of 60 L/h of permeate from first stage with membrane NF90-2540 at 40 bar and an initial conductivity of 1,700 µS/cm.

Table 6
TDS, sodium chloride, chloride, and sodium ion retention with ionic exchange columns (Purolite A-300 and Purolite C-100) with a feed flow of 20 L/h of permeate from first stage with membrane NF90-2540 at 40 bar

	Feed	Exit	Retention (%)	NCH 409	OMS
TDS (mg/L)	853	53.7	94	1,500	1,000
NaCl (mg/L)	853	53.7	94	–	–
Cl^- (mg/L)	517.6	32.6	94	400	250
Na^+ (mg/L)	335.4	21.1	94	–	100

Table 7
TDS, sodium chloride, chloride, and sodium ion retention with ionic exchange columns (Purolite A-300 and Purolite C-100) with a feed flow of 60 L/h of permeate from first stage with membrane NF90-2540 at 40 bar

	Feed	Discharge	% Retention	NCH 409	WHO
TDS (mg/L)	853	107.2	87.4	1,500	1,000
NaCl (mg/L)	853	107.2	87.4	–	–
Cl^- (mg/L)	517.6	65.1	87.4	400	250
Na^+ (mg/L)	335.4	42.1	87.4	–	100

Fig. 11 shows that the stationary state is achieved in about 10 min with an average conductivity of approximately 214 µS/cm, which indicates low salt content present in the output water.

In Tables 6 and 7 it can be observed that increasing the feed flow, increases the concentration of salts output where, for a flow of 60 L/h is obtained a product with a concentration of 107.2 mg/L TDS, whereas for a flow of 20 L/h, the output concentration decreases to 53.7 mg/L, which represents a significant concentration decreased with decreasing flow, whereby low feed streams are suggested to achieve greater exchange of ions.

4. Conclusions

(1) It is possible to obtain drinking water from seawater with a two-stage process involving nanofiltration and ion-exchange technologies. Experimental results show that it is possible to obtain salts rejection yield of a 99.9% using two stages of nanofiltration at transmembrane pressures (TMP) 40 and 20 bars, respectively, temperature of 15°C, and feed flow 707 L/h. It is also possible to obtain a 95% yield of salt rejection using a combined process with a first

stage of nanofiltration and a second stage using ionic exchange resins. The second option represents smaller energy consumption, because of the lower operation pressures. Both methods fulfill the current Chilean drinking water standard (NCh 409).

(2) Nanofiltration membranes produce a much higher permeate flow (over three times permeate flow) than RO membranes at same operation conditions.

(3) Ionic exchange process increase salts adsorption rate with a low feed flow and a low feed conductivity. Nevertheless, the process was able to overcome Chilean drinking water standard with the most adverse operating conditions (feed flow and conductivity of 60 L/h and 1,707 μS/cm, respectively).

Acknowledgments

This study received financial support from CONICYT/FONDAP Grant 15130015.

References

[1] Library of National Congress of Chile, The Shortage of Fresh Water, 2006. Available from: <http://www.bcn.cl/carpeta_temas/temas_portada.12-27.4449440028>.

[2] R.K. Pachauri, A. Reisinger, Climate Change, Climate Change 2007: Synthesis Report, Intergovernmental panel on climate change, Geneva, Switzerland, 2007, pp. 104.

[3] K. Betts, Technology solutions: Desalination, desalination everywhere, Environ. Sci. Technol. 38(13) (2004) 246A–247A.

[4] M.A. Shannon, P.W. Bohn, M. Elimelech, J.G. Georgiadis, B.J. Mariñas, A.M. Mayes, Science and technology for water purification in the coming decades, Nature 452(7185) (2008) 301–310.

[5] L.F. Greenlee, D.F. Lawler, B.D. Freeman, B. Marrot, P. Moulin, Reverse osmosis desalination: Water sources, technology, and today's challenges, Water Res. 43(9) (2009) 2317–2348.

[6] H.K. Shon, S. Vigneswaran, J. Cho, Comparison of physico-chemical pretreatment methods to seawater reverse osmosis: Detailed analyses of molecular weight distribution of organic matter in initial stage, J. Membr. Sci. 320(1–2) (2008) 151–158.

[7] T. Matsuura, Progress in membrane science and technology for seawater desalination—A review, Desalination 134(1–3) (2001) 47–54.

[8] M. Elimelech, W.A. Phillip, The future of seawater desalination: Energy, technology, and the environment, Science 333(6043) (2011) 712–717.

[9] A. Subramani, M. Badruzzaman, J. Oppenheimer, J.G. Jacangelo, Energy minimization strategies and renewable energy utilization for desalination: A review, Water Res. 45(5) (2011) 1907–1920.

[10] R. Semiat, Energy issues in desalination processes, Environ. Sci. Technol. 42(22) (2008) 8193–8201.

[11] M. Chillón Arias, L. Valero i Bru, D. Prats Rico, P. Varó Galvañ, Approximate cost of the elimination of boron in desalinated water by reverse osmosis and ion exchange resins, Desalination 273 (2011) 421–427.

[12] E. Swyngedouw, Into the sea: Desalination as hydro-social fix in Spain, Ann. Assoc. Am. Geogr. 103(2) (2013) 261–270.

[13] A. Criscuoli, E. Drioli, Energetic and exergetic analysis of an integrated membrane desalination system, Desalination 124 (1999) 243–249.

[14] A. Hassan, M. Al-Sofi, A. Al-Amoudi, A. Jamaluddin, A. Farooque, A. Rowaili, A. Dalvi, N. Kither, G. Mustafa, I. Al-Tisan, A new approach to membrane and thermal seawater desalination processes using nanofiltration membranes (Part 1), Desalination 118 (1998) 35–51.

[15] N. Hilal, H. Al-Zoubi, N.A. Darwish, A.W. Mohamma, A comprehensive review of nanofiltration membranes: Treatment, pretreatment, modelling, and atomic force microscopy, Desalination 170 (2004) 281–308.

[16] W. Bowen, H. Mukhtar, Characterisation and prediction of separation performance of nanofiltration membranes, J. Membr. Sci. 112 (1996) 263–274.

[17] J. Schaep, B. Van der Bruggen, C. Vandecasteele, D. Wilms, Influence of ion size and charge in nanofiltration, Sep. Purif. Technol. 14 (1998) 155–162.

[18] M. Afonso, G. Hagmeyer, R. Gimbel, Streaming potential measurements to assess the variation of nanofiltration membranes surface charge with the concentration of salt solutions, Sep. Purif. Technol. 22–23 (2001) 529–541.

[19] D.X. Vuong, Two Stage Nanofiltration seawater desalination system, United State Patent 7, 144, 511 B2, December 2006.

[20] J.S. Zhou, G.W. Chen, Development of nanofiltration membrane, Membr. Sci. Technol. 19(4) (1999) 1–116.

[21] K. Abdullaev, M. Agamaliev, V. Kosmodamianskii, O. Dadashova, Substantiation of flow charts for reverse-osmosis desalting with the ion-exchange softening of sea water and permeate, J. Water Chem. Technol. 32 (3) (2010) 187–192.

[22] R. Treybal, Mass Transfer Operations, third ed., McGraw-Hill Bok Company, New York, NY, 1988.

[23] J.M. Coulson, J.F. Richardson, Ion Exchange, Chemical Engineering, vol. 2, Bath Press, Bath, 2002, pp. 1053–1075.

[24] Hanna Instruments, Chemical Composition of Sea Water, 2008. Available from: <http://www.hannachile.com/noticias-articulos-y-consejos/articulos/item/246-el-agua-de-mar>.

[25] C.O. Anne, D. Trébouet, P. Jaouen, F. Quemeneur, Nanofiltration of seawater: Fractionation of mono and multivalent cations, Desalination 140(1) (2001) 67–77.

[26] M. Pontie´, C. Diawara, M. Rumeau, D. Aureau, P. Hemmery, Seawater nanofiltration (NF): Fiction or reality? Desalination 158 (2003) 277–280.

[27] M. Pontié, A. Lhassani, C.K. Diawara, A. Elana, C. Innocent, D. Aureau, M. Rumeau, J.P. Croue, H. Buisson, P. Hemery, Seawater nanofiltration for the elaboration of usable salty waters, Desalination 167(1–3) (2004) 347–355.